PERGAMON

Deep-Sea Research I 48 (2001) 1093–1120

DEEP-SEA RESEARCH
PART I

www.elsevier.com/locate/dsr

Ascending and descending particle flux from hydrothermal plumes at Endeavour Segment, Juan de Fuca Ridge

James P. Cowen[a,*], Miriam A. Bertram[a,1], Stuart G. Wakeham[b], Richard E. Thomson[c], J. William Lavelle[d], Edward T. Baker[d], Richard A. Feely[d]

[a]*Department of Oceanography, University of Hawaii, 1000 Pope Road, Honolulu, Hawaii 96822, USA*
[b]*Skidaway Institute of Oceanography, 10 Ocean Science Circle, Savannah, Georgia 31411, USA*
[c]*Department of Fisheries and Oceans, Institute of Ocean Sciences, 9860 West Saanich Road, Sidney, BC, Canada V8L 4B2*
[d]*Pacific Marine Environmental Laboratory, National Oceanographic and Atmospheric Administration, 7600 Sand Point Road NE, Seattle, WA 98115, USA*

Received 22 April 1999; received in revised form 19 June 2000; accepted 21 July 2000

Abstract

Bio-acoustic surveys and associated zooplankton net tows have documented anomalously high concentrations of zooplankton within a 100 m layer above the hydrothermal plumes at Endeavour Segment, Juan de Fuca Ridge. These and other data suggest that congregating epi-plume zooplankton are exploiting a food substrate associated with the hydrothermal plume. Ascending, organic-rich particles could provide a connection. Consequently, two paired sequentially sampling ascending and descending particle flux traps and a current meter were deployed on each of three moorings from July 1994 to May 1995. Mooring sites included an on-axis site (OAS; 47°57.0′N, 129°05.7′W) near the main Endeavour vent field, a "down-current" site 3 km west of the main vent field (WS), and a third background station 43 km northeast of the vent field (ES). Significant ascending and descending particle fluxes were measured at all sites and depths. Lipid analyses indicated that ascending POC was derived from mid-depth and deep zooplankton whereas descending POC also contained a component of photosynthetically derived products from the sea surface. Highest ascending POC fluxes were found at the hydrothermal plume-swept sites (OAS and WS). The limited data available, however, precludes an unequivocal conclusion that hydrothermal processes contribute to the ascending flux of organic carbon at each site. Highest ascending to descending POC flux ratios were also found at WS. Observed trends in POC, PMn/PTi, and PFe/PTi clearly support a hydrothermal component to the descending flux at the plume-swept WS site (no descending data was recovered at OAS) but not at the

* Corresponding author. Tel.: + 1-808-956-7124; fax: + 1-808-956-9225.
[1] Present address: PMEL, NOAA, 7600 Sand Point Road NE, Seattle, WA 98115, USA.
E-mail address: jcowen@soest.hawaii.edu (J.P. Cowen).

PII: S0967-0637(00)00070-4

background ES site. Alternative explanations for ascending particle data are discussed. First-order calculations for the organic carbon input (5–22 mg C m^{-2} d^{-1}) required to sustain observed epi-plume zooplankton anomalies at Endeavour are comparable both to measured total POC flux to epi-plume depths (2–5 mg C m^{-2} d^{-1}: combined hydrothermal and surface derived organic carbon) and to estimates of the total potential in situ organic carbon production (2–9 mg C m^{-2} d^{-1}) from microbial oxidation of hydrothermal plume H_2, CH_4 and NH_4^+.

Keywords: Hydrothermal plumes; Organic carbon production; Ascending/descending flux; Endeavour Segment; Juan de Fuca Ridge

1. Introduction

Hydrothermal vent plumes are the pathways through which energy and mass flow between the geophysical processes controlling crustal accretion and the overlying ocean waters. Considerable research has been conducted on the effects of hydrothermal venting on benthic fauna and on bacteria in the benthos and laterally spreading plumes (e.g., Wiebe et al., 1988; Van Dover and Fry, 1989; see Tunnicliffe, 1991). Geochemical studies of the transformation, lateral dispersion and ultimate removal of hydrothermal chemical constituents have also emphasized the immediate vent field environment (see Von Damm, 1990) and the buoyant and non-buoyant plumes (e.g., Bolger et al., 1978; Lupton et al., 1980; Cowen et al., 1986, 1990; Klinkhammer and Hudson, 1987; Dymond and Roth, 1988; Roth and Dymond, 1989; Feely et al., 1992, 1994). Until recently, however, little attention had been given to the potential influence that hydrothermal venting might have on secondary productivity in the water column at levels above the reach of the buoyant and neutrally buoyant plumes (Thomson et al., 1988, 1989, 1991, 1992a; Burd et al., 1992; Lavelle et al., 1992; Cowen et al., 1998).

Essentially yearly bio-acoustic surveys (1987–1996) have revealed substantial scattering layers consistently overlying hydrothermal plumes found above the central (Main) vent field of the Endeavour Segment, northern Juan de Fuca Ridge (Thomson et al., 1988, 1989, 1991, 1992a; Thomson, unpublished data). Associated net tows have documented anomalously high (10–100 times background levels) concentrations of zooplankton within the 100 m scattering layer (1800–1900 m) immediately above the top of the neutrally buoyant plume, about 200–300 m above the sea floor (Burd et al., 1992; Thomson et al., 1992a). The acoustic tows show that this deep scattering layer typically overlies the surface that marks the maximum rise height of the plumes emanating from the main endeavour field (MEF) at the central ridge (Thomson et al., 1992a). In contrast, bioacoustical measurements and zooplankton net tows within the hydrothermal plume itself at depths of 2000–2200 m were below background levels suggesting that the zooplankton avoid the plume itself (Burd et al., 1992; Thomson et al., 1992a).

Enhanced (four-fold) vertically integrated biomass and unusual species and life-stage compositions associated with the epi-plume acoustic/net tow zooplankton anomalies (Burd and Thomson, 1993) strongly suggest that the congregating zooplankton are exploiting an enhanced food source associated with the hydrothermal system. Roth and Dymond (1989) calculated that most of the organic carbon collected in a particle trap deployed within the hydrothermal plume at Endeavour is produced chemosynthetically. Thus POC production within hydrothermal vent fields

and resulting plumes might support the observed epi-plume zooplankton biomass anomalies, contingent on a delivery mechanism between the zooplankton-scarce zone within the plumes and the zooplankton-rich zones above the plume.

Ascending, organic-rich particles could provide the connection. Yayanos and Nevenzel (1978) first considered the possible existence of an ascending particle flux. Recent studies have documented such a process in the deep ocean, showing that the magnitude of ascending fluxes may be a significant fraction of descending fluxes (Simoneit et al., 1986; Smith et al., 1989; Grimalt et al., 1990). Measured ratios of ascending to descending particle flux varied from 1 to 4% for total mass flux (Simoneit et al., 1986) and 1–66% for POC (Smith et al., 1989), depending on station and season.

This paper describes a study of both ascending and descending particle flux at an active ridge crest spreading center. We were particularly concerned with the influence of venting on the background fluxes. Analyses consisted of total particulate material (TPM), particulate organic carbon (POC), nitrogen (PN), and lipids, and particulate Mn, Fe, and Ti (PMn, PFe, PTi). The potential carbon and mineral linkages between hydrothermal venting and the deep and mid-depth ocean water column are the focus of the present paper.

2. Site description and methods

The study site was centered over the main vent field (MEF) of the Endeavour Segment of the Juan de Fuca Ridge (48.9°N, 129.1°W) (Fig. 1). The Endeavour Segment is a 300 km long, 10 km wide, north–south trending crustal feature at the northern end of the Juan de Fuca Ridge, approximately 300 km west of Washington state. Four active vent fields have now been documented on the Endeavour Segment (Delaney et al., 1992, 1997; Thomson et al., 1992b; Robigou et al., 1993; Lilley et al., 1995). These vent fields are within a 100 m deep axial valley at an approximate depth of 2200 m.

Three bottom-moored arrays were deployed in July of 1994 from the *CFAV Endeavour* and recovered in May, 1995, by the *RV Surveyor*. Each array was equipped with two paired particle flux traps. Each trap pair (Fig. 2) included one conventional "PMEL-type" (Baker and Milburn, 1983) trap (descending particle trap) and one inverted "modified PMEL" ascending particle trap. Traps were not specifically calibrated and their collection efficiency is not known. However, the overall trap designs (cylindrical traps with high length-to-width ratios, collection cylinders closed during deployment/recovery) and mooring configuration (short, bottom-moored) in a relatively low-energy environment provide favorable trapping conditions (Knauer and Asper, 1989; Gust et al., 1994).

Deployment locations, times, and depths are listed in Table 1. The deep trap pair was positioned to coincide with the middle of the typical neutrally buoyant plume at Endeavour Segment, whereas the "shallow" trap pair was positioned ~ 150 m above the nominal upper plume boundary. An Aanderra RCM-5 current meter was also deployed on each mooring, approximately midway between the deep and shallow particle traps (Table 1). The "on-axis" mooring (OAS) was located near the MEF within the axial valley. The "West" mooring was placed approximately 3 km west of the MEF site. Previous water column surveys indicated that this West mooring site (WS) should be within the typical down-stream path of the hydrothermal plume which is laterally advected from the Endeavour vent fields. A third mooring, about 43 km east (ES) of the Endeavour Segment, constituted a background site chosen to be free of significant hydrothermal influence.

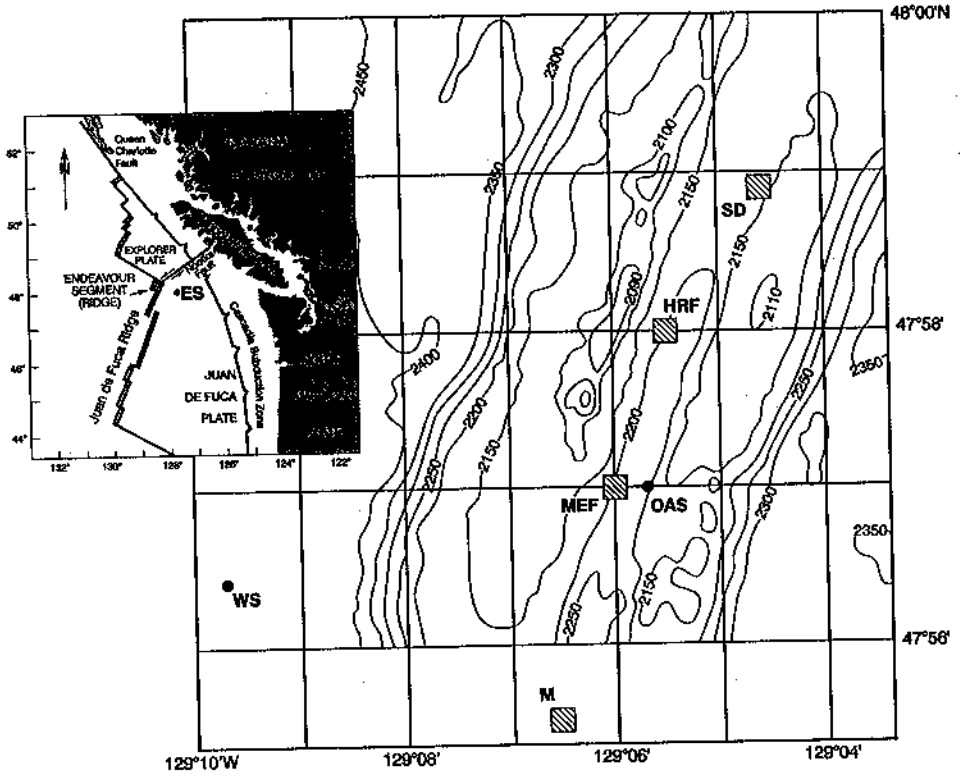

Fig. 1. Map showing positions of particle trap moorings on the axis and flanks of the Endeavour Segment. Inset shows the Endeavour Segment with respect to the Juan de Fuca Ridge and northeast Pacific; East mooring Site (ES) is indicated in inset. Moorings are indicated with filled circle; vent fields with hatched squares (Salty Dawg, SD; High Rise Field, HRF; Main Endeavour Field, MEF). Bathymetry is in meters.

Traps collected samples in a sequence of 10 33-day intervals. Collection cylinders were poisoned with sodium azide in a slightly positively (or negatively) buoyant solution for the ascending (or descending) particle traps, respectively. Ascending particle traps were specially adapted to minimize the potential loss of particles that may loose their positive buoyancy prior to the end of a cylinder's 33-day open collection interval (Fig. 2b). Basically, a cone in the top end of the cylinder deflects rising particles to the perimeter of the cylinder so that any subsequent loss of particle buoyancy would result in the particles falling into the collection-well rather than out of the cylinder through the tapered entrance.

Upon mooring recovery, trap collection cylinders were iced until processed on shore. Within 5 days of recovery, samples were pre-screened through clean 1 mm mesh Nitex and split with a high-precision splitter (Tennant and Baker, 1987) into fractions for gravimetric, carbon and nitrogen, lipid, and major element (XRF) analyses. Each collection cylinder for the descending traps was processed separately. However, since ascending particle trap collections were considerably smaller, sequential pairs of ascending particle collection cylinders were combined during the splitting operation producing bimonthly sampling intervals. Sub-samples were temporarily stored

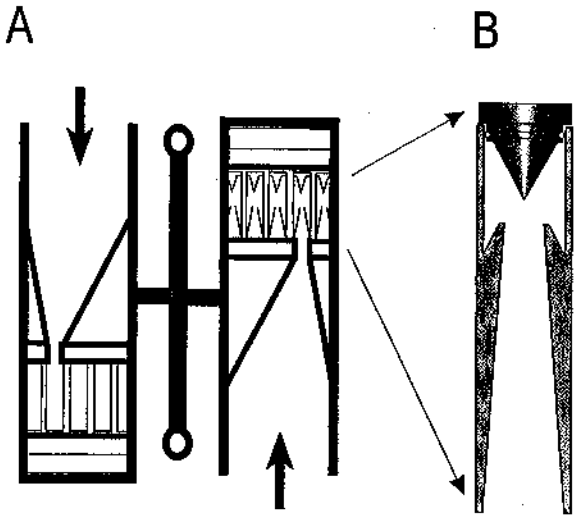

Fig. 2. (A) Schematic of the ascending and descending particle trap pairs, consisting of a conventional descending PMEL-type trap (Baker and Milburn, 1983) and a second PMEL-type trap slightly modified for collection of ascending particles. (B) Detail of ascending trap collection cup.

under refrigeration in either polypropylene tubes or combusted glass bottles (lipid samples). The solute phases of our trap collection cylinder solutions were not analyzed. Since captured sinking particles can leach organic material and metals into trap solutions (Knauer et al., 1984), the particle flux values reported must be considered to be at the lower bound of the actual in situ flux (Karl et al., 1996). Few swimmers were found in descending or ascending traps. No significant variability in swimmer abundance was noted and all visible zooplankton were removed prior to splitting. Filters of splits used for gravimetric measurements were examined by light microscopy, revealing generally amorphous material with occasional small egg-like particles.

Separate sub-samples for particulate carbon (PC) and nitrogen (PN) and lipid analyses were filtered through combusted glass fiber filters (GFF). PC and PN were determined with a Europa Scientific 2400 CN analyzer, using an extended standard curve of ~ 50 to 5,000 μg acetanilide (Aldrich Chemical Co., Inc.). An estimate of POC was calculated by subtracting the $CaCO_3$–carbon fluxes from the total carbon fluxes; Ca concentrations obtained by XRF were used to obtain an estimate of the $CaCO_3$.

Lipids in trap samples were extracted with methylene-chloride : methanol (2 : 1) and saponified to separate neutral lipids from acids (Wakeham and Canuel, 1988). Neutral lipid fractions were derivatized with BSTFA/pyridine and acids were methylated with diazomethane. Fractions were analyzed by gas chromatography on a Carlo Erba Fractovap 6800 using a 60 m DB-05 capillary and hydrogen as carrier gas. Internal standards were added for quantification. Gas chromatography-mass spectrometry was conducted with a Hewlett-Packard 5890II/Finnigan Incos 50 GC/MS system and the same column but with helium as the carrier gas.

Total elemental composition of the particulate matter was determined by X-ray primary- and secondary-emission spectrometry with a Kevex Model 8000-770 X-ray energy spectrometer with a rhodium X-ray source and Mo, Ti, Se, and Co secondary targets and a non-destructive thin film

Table 1
Mooring positions, collection dates, and trap and current meter depths

Mooring site	Latitude	Longitude	Instrument depth			Collection dates	
				(m)	(mab)	Start	End
West flank	47°56.4′N	129°9.7′W	Trap-shallow	1690	714	07/27/94	04/17/95
			Trap-deep	2040	364	07/27/94	04/17/95
			Current meter	1840	564	07/27/94	05/14/95
On-axis	47°57.0′N	129°5.7′W	Trap-shallow	1661	479	07/21/94	05/14/95
			Trap-deep	2010	130	07/21/94	05/14/95
			Current meter	1811	329	07/21/94	05/14/95
East flank	48°7.5′N	128°21.1′W	Trap-shallow	1637	973	07/15/94	05/08/95
			Trap-deep	1986	624	07/15/94	05/08/95
			Current meter	1786	724	07/15/94	05/15/95

technique (Baker and Piper, 1976; Holmes, 1981; Feely et al., 1991). Precision was approximately 2% for Ti, Mn, and Fe.

The water column near the traps was also sampled with a CTD-transmissometer 301 Niskin bottle (General Oceanics) rosette package. Ammonium sample preparation is discussed in Cowen et al. (1998) after Jones (1991). Trace metal samples were drawn directly into specially acid-cleaned 250-ml linear polyethylene bottles and stored at room temperature until processed. On shore, trace element samples were acidified (pH < 2) several weeks prior to analysis. Total dissolvable manganese concentrations were determined by a flow injection analysis technique with on-line preconcentration and spectrophotometric detection (Resing and Mottl, 1992). Methane samples were drawn into combusted 230 ml glass serum bottles (Kimble), poisoned with 1 ml supersaturated $HgCl_2$ solution, and capped with butyl rubber septa secured with an aluminum crimp-seals. Methane concentrations and carbon isotopic composition were determined with an isotope-ratio-monitor gas-chromatography/mass-spectrometry method (Popp et al., 1995; Sansone et al., 1997). The detection limit for this system is 200 pmol of CH_4 in solution. Methane carbon isotopic data will be reported elsewhere.

3. Results

The mass flux and geochemical data confirm that the location of the moorings with respect to plume presence or absence was as intended: OAS and WS were situated in locations subject to the presence of hydrothermal plumes, but ES was not. Light transmission and temperature anomaly ($\Delta\theta$) data (Fig. 3) confirm that the on-axis (OAS) and West flank site (WS) moorings were within the path of the laterally advected hydrothermal plume. Near-bottom maxima in both signals indicate the depth of the plume to be between 1950 and 2200 m. There also were large maxima in manganese (> 90 nM), methane (598 nM) and ammonium (400 nM) within on-axis plume depths (Figs. 4 and 5), consistent with nearby hydrothermal sources. The WS plume was weaker but clearly present as

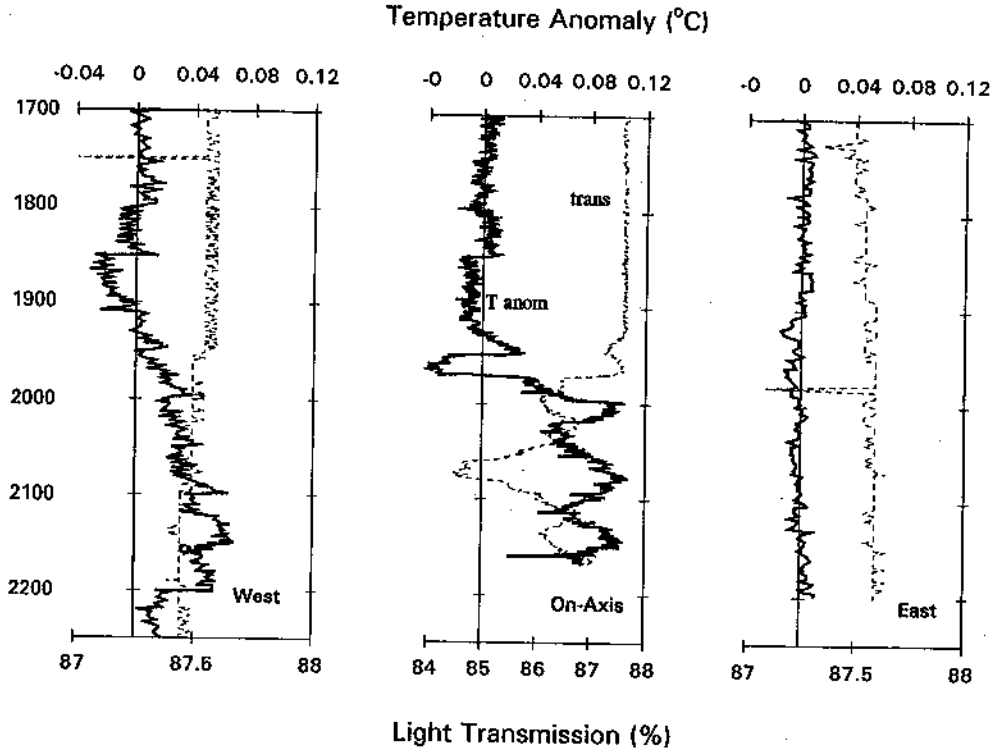

Fig. 3. Vertical profiles for temperature anomaly (heavy linge) and light transmission (light line) at representative stations near the on-axis, West, and East site moorings.

evidenced by small anomalies in temperature, light transmission, and concentrations of Mn, CH_4, and NH_4. No hydrothermal signal was observed at the background East mooring site (ES) (Figs. 3–5).

The vent-specific origin of the plume material at WS and OAS cannot be precisely specified. Nevertheless, OAS plumes are likely dominated by emissions from the nearby MEF. However, in general the current data suggest that the plume likely follows a meandering path from the vent fields to WS (Thomson et al., 1998; Mihaly et al., 1998). There was a northerly advection superimposed over the mean southwest flow, and tidal and inertial currents helped to disperse the plumes. In fact, WS could be exposed to plumes originating from any of the extant Endeavour vent fields. Four high-temperature hydrothermal fields have been described along the Endeavour Segment of the Juan de Fuca Ridge with average spacing of 1.9 ± 0.3 km (Robigou et al., 1993; Lilley et al., 1995; Veirs et al., 1996; Delaney et al., 1997). Although each field is distinctive in terms of geological setting and sulfide deposition characteristics (Delaney et al., 1997), the vent fluids from the four fields appear to be generally similar in composition with regard to key gas and ion chemistry (M. Lilley, personal communication). Under conditions of weak mean flow, the higher-frequency motion observed in the current data could quite easily disperse the plume to the West site from any of these fields.

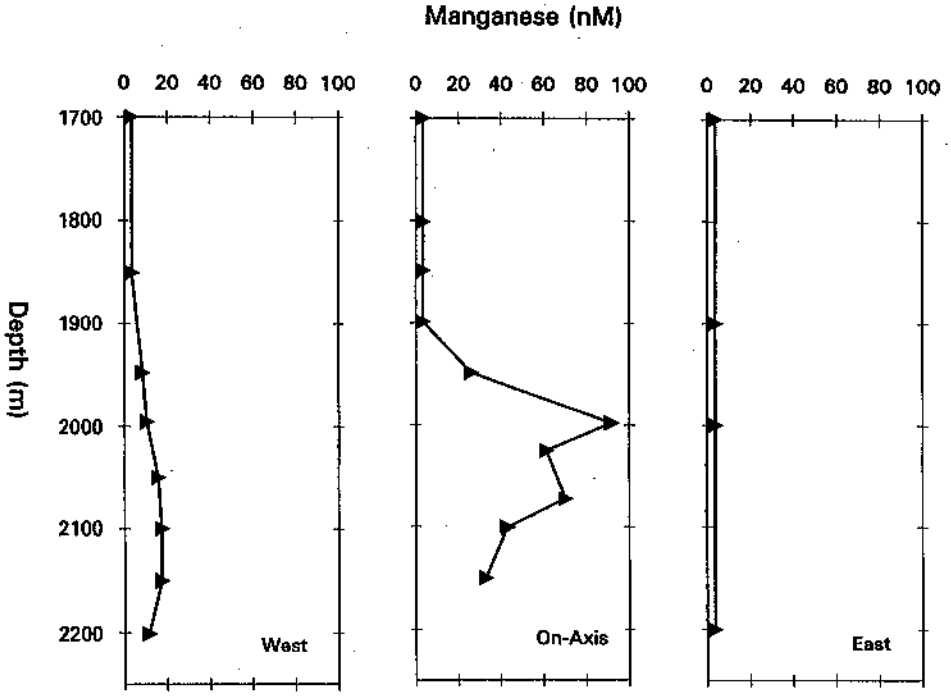

Fig. 4. Vertical profiles for total dissolvable manganese at representative stations (as in Fig. 3) near the on-axis, West, and East site moorings.

The spatial and temporal dynamics of mid-ocean ridge (MOR) hydrothermal plumes must be considered. True time-integrated, plume-depth backgrounds are very difficult or impossible to obtain near the Endeavour ridge. The spatial footprint of the hydrothermal plume is on the order of 10 s to 100 s km or more in diameter. The plumes are wafted about by tidal as well as shifting "prevailing" currents (Cannon and Pashinski, 1997; Wetzler et al., 1998). Consequently, off-axis plumes represent moving targets and even time-integrated samples such as derived from particle flux traps are susceptible to large variances.

3.1. *Particle flux traps*

Where possible, flux data were analyzed with a two sample *t*-test. In such cases, "*p*" values are given, as is an indication of whether equal or unequal sample variance statistics were used.

3.1.1. *Total particulate material*

Total particulate material (TPM) fluxes are plotted in Fig. 6; average values are listed in Table 2. Average ascending TPM fluxes were highest at OAS (0.83–0.85 mg m^{-2} d^{-1}), with lower values at the WS (0.27–0.54 mg m^{-2} d^{-1}) and ES (0.34–0.47 mg m^{-2} d^{-1}) (Table 2). The ascending fluxes at OAS were significantly ($p < 0.08$, unequal var.) greater than at WS. Both shallow and deep descending TPM fluxes were generally higher at the more coastal ES (27.9–30.2 mg m^{-2} d^{-1}) than

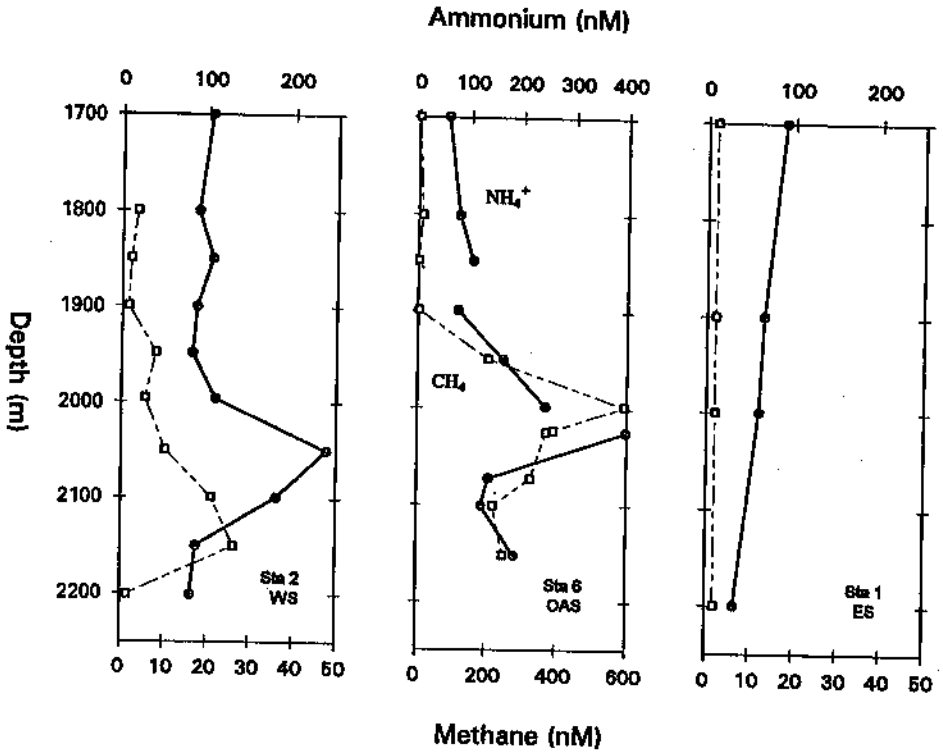

Fig. 5. Vertical profiles for ammonium (circles) and methane (squares) concentrations at representative stations (as in Fig. 3) near the on-axis, West, and East site moorings.

at the WS (6.0–25.5 mg m^{-2} d^{-1}) (Table 2); only shallow mean differences were significant ($p < 0.001$, equal var.). Deep descending WS fluxes were consistently greater than shallow descending fluxes ($p < 0.018$, equal var.). Average ratios of ascending to descending TPM fluxes were greater for WS shallow traps than for deep WS or for either shallow or deep ES traps (Table 2). The controllers of both the shallow and deep descending traps at the on-axis site failed to operate properly. The ratio calculated for the shallow WS trap samples was more than 4 times greater than for either the shallow or deep ES traps, reflecting both the larger descending and smaller ascending fluxes measured there.

3.1.2. *Particulate carbon and nitrogen*

In order to insure accurate CN analysis of ascending particle flux samples, aliquots from sequential collection cylinders from individual ascending traps were usually pooled further (Table 2). Consequently, in most cases the ascending CN data represent average values for multiple collection intervals, precluding meaningful statistical analyses. In a number of instances average POC fluxes exceeded corresponding TPM fluxes. This is primarily because of splitting errors and because the ascending fluxes are small relative to descending fluxes, and the ascending particles are essentially entirely lipid-rich organics with only traces of other organic material.

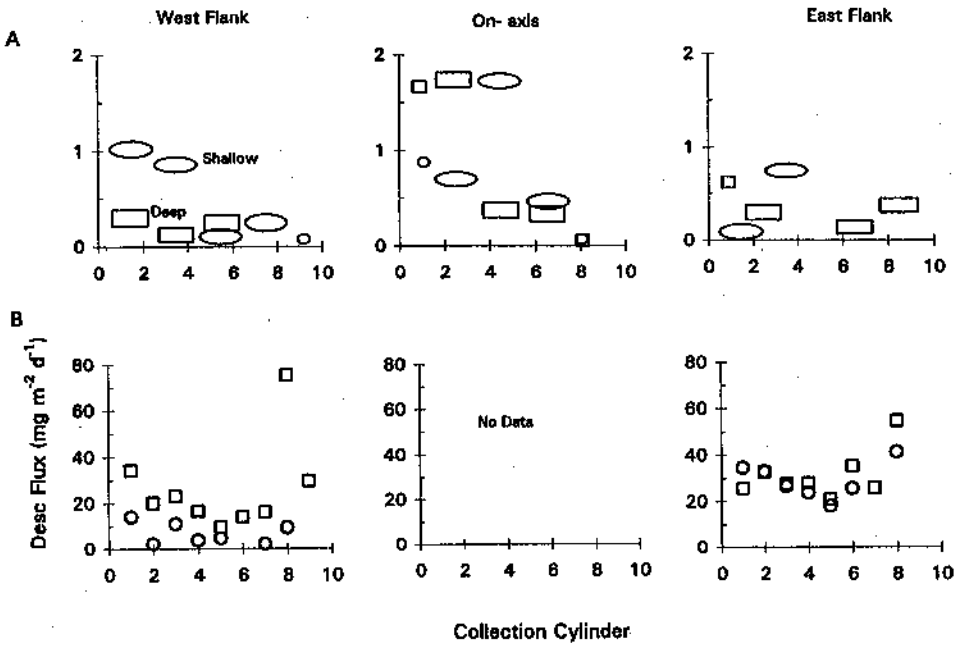

Fig. 6. Time-series total particulate material (TPM) fluxes to the shallow (circles, ovals) and deep (squares, rectangles) particle traps moored at the West, on-axis, and East mooring sites: (A) ascending flux; (B) descending flux. Ovals and rectangles represent pooled collection intervals.

Ascending POC flux was greater at shallow depths than at deep depths for each site (Fig. 7a), with the highest shallow ascending fluxes at OAS followed by WS. Average deep ascending fluxes were also slightly greater at OAS and WS than at ES. The difference between the shallow and deep ascending POC flux is greatest at OAS, though similar between WS and ES (Fig. 7d). In contrast to the ascending fluxes, the descending POC fluxes at ES were generally larger than at WS (Fig. 7b). It is notable, however, that the measured deep descending POC flux at WS was consistently greater than the corresponding shallow flux (shallow : deep flux ratio < 0.5; Fig. 7d); the mean deep descending flux was significantly greater than the shallow flux (2 sample t-test, $p < 0.03$, equal var.). On the other hand, a consistent pattern in relative shallow and deep descending fluxes was absent at ES (Fig. 7b), although the shallow : deep ratio was higher at ES (0.5 to > 2) than at WS (< 1) for all collection intervals (Fig. 7d). The ascending: descending POC-flux ratios are dramatically higher at WS than at the background ES, because of both higher ascending and lower descending fluxes at WS (Fig. 7c). The trends in PN flux are similar to those of the POC-flux (Table 2).

3.1.3. *Lipid fluxes*

Lipid fluxes will be discussed in detail separately. Because we were unsure of the amount of lipid in the time series samples, all collection cylinders from individual particle flux traps were pooled for this first round of lipid analyses, yielding a single sample per trap. Distinct differences in lipid flux are evident between OAS and WS traps on the one hand and the background ES traps on the other

Table 2
Average ascending and descending fluxes for total particulate material, particulate organic carbon, particulate nitrogen, particulate Mn/Ti, and particulate Fe/Ti

Mooring site	Trap depth (m)	TPM			POC			PN			PMn/Pti		PFe/PTi	
		Ascend.	Descend.	Asc./Desc. (ratio)	Ascend.	Descend.	Asc./Desc. (ratio)	Ascend.	Descend.	Asc./Desc. (ratio)	Ascend.	Descend.	Ascend.	Descend.
		($mg\,m^{-2}\,d^{-1}$)			($mg\,m^{-2}\,d^{-1}$)			($mg\,m^{-2}\,d^{-1}$)			(mol ratio)		(mol ratio)	
West (WS)	1690	0.54	6.0	0.09	0.73	0.84	0.87	0.057	0.14	0.47	0.42	0.22	13.5	11.9
	2040	0.27	25.5	0.01	0.39	2.0	0.20	0.048	0.20	0.67	0.44	0.63	14.5	22.1
On-axis (OAS)	1661	0.85	—[a]	—	0.92	—	—	0.088	—	—	0.26	—	9.7	—
	2010	0.83	—	—	0.45	—	—	0.050	—	—	0.49	—	27.4	—
East (ES)	1637	0.47	27.9	0.02	0.56	4.1	0.14	0.075	0.55	0.12	0.34	0.16	13.3	10.7
	1986	0.34	30.2	0.01	0.21	3.0	0.07	0.033	0.37	0.10	0.32	0.27	11.8	10.6

[a]"—"denotes no data.

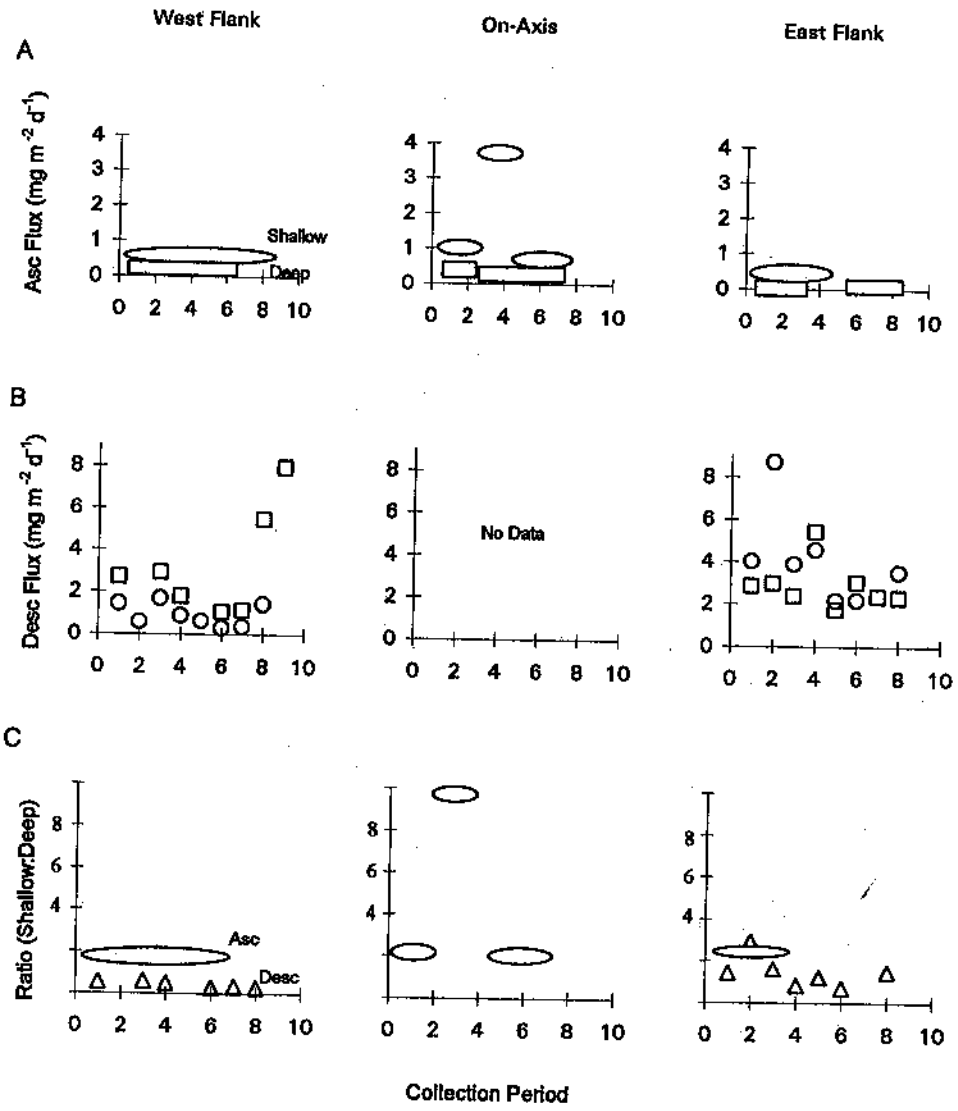

Fig. 7. Time-series particulate organic carbon (POC) fluxes to the shallow (circles, ovals) and deep (squares, rectangles) particle traps moored at the West, on-axis, and East mooring sites: (A) ascending flux; (B) descending flux; (C) ratios of shallow: deep fluxes for ascending (diamonds) and descending (triangles) fluxes. Ovals and rectangles represent pooled collection intervals.

(Fig. 8a). At WS, the ascending lipid flux was higher than the descending lipid flux for each lipid class (neutrals, acids, and total). At OAS and WS, the ascending lipid flux above the upper boundary of the plume (shallow traps) was 3–5 times higher than the deep ascending lipid flux and 4–8 times higher than the WS descending lipid flux. The highest lipid flux for all traps was the ascending flux to the shallow OAS trap. Although the ascending lipid flux to the shallow ES trap is

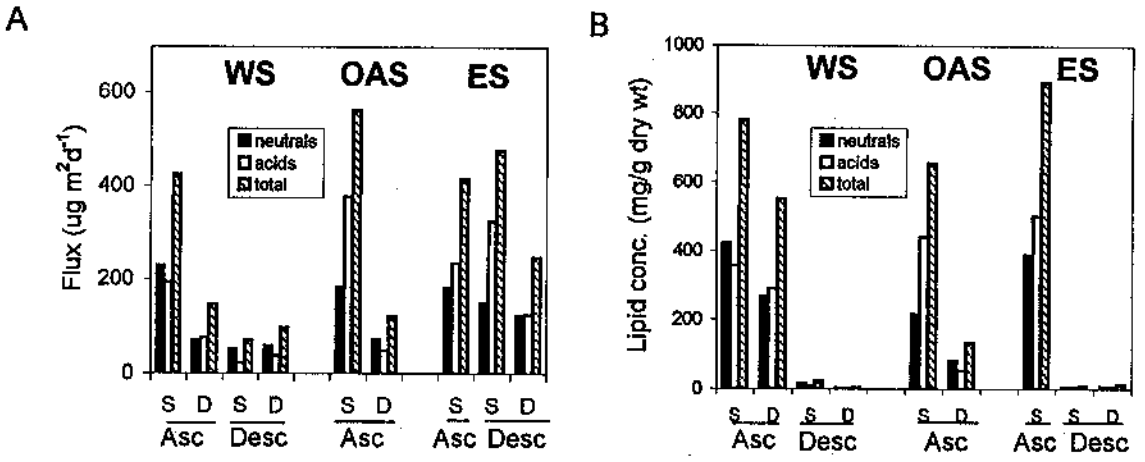

Fig. 8. (A) Ascending and descending fluxes of major lipid classes; (B) concentrations of same lipid classes in trap materials. Neutrals (black), acids (white), and total (lined). Shallow and deep traps are indicated by 'S' and 'D'; 'WS', 'OAS', and 'ES' indicate West, on-axis, and East (background) mooring sites.

comparable to that of the shallow WS trap, both the shallow and deep descending lipid flux at the ES were considerably higher than the WS descending flux. This comparison of lipid fluxes contrasts markedly with TPM and POC, for which descending fluxes were generally higher than ascending fluxes.

Ascending particles were significantly enriched in lipids. Lipid concentrations (mg lipid/g dry TPM) were over an order of magnitude higher in the ascending particles than in the descending particles (Fig. 8b). Lipid concentrations were also somewhat higher in the shallow traps than in the deep traps, and higher in the WS ascending particle traps than at OAS. The major lipids in the traps were fatty acids (derived largely from wax esters), sterols, fatty alcohols (from wax esters) and alkenones. There were clear differences in the distribution of many lipid classes between the descending and ascending particle flux samples including neutral lipids and fatty acids (Fig. 9). Sterols, for example, tend to be enriched in descending particle trap samples (17–26% of total lipid) but depleted in ascending particle samples (1–3%). By contrast, fatty alcohols were generally slightly enriched in ascending particles (20–55%) compared to descending particles (17–45%) although overlap was present. Zooplankton-derived wax esters were indicated by the fact that the most abundant fatty acids and alcohols tended to be 20:1 and 22:1 monounsaturated molecules. Zooplankton-derived cholesterol was the dominant sterol in ascending particles. A mixture of phytosterols and long-chain alkenones were found only in the descending particle samples, consistent with a surface-water phytoplankton source. Thus ascending particles are dominated by lipids derived from mid-water zooplankton (Wakeham et al., 1984) inhabiting the region of the plume (Comita et al., 1984) while descending particles represent a mixture of lipids originating in surface waters and near the plume. Our observations of enhanced ascending lipid fluxes and different compositions between ascending and descending particles associated with the hydrothermal plume complement earlier results for open ocean regions in the Pacific and Atlantic (Grimalt et al., 1990).

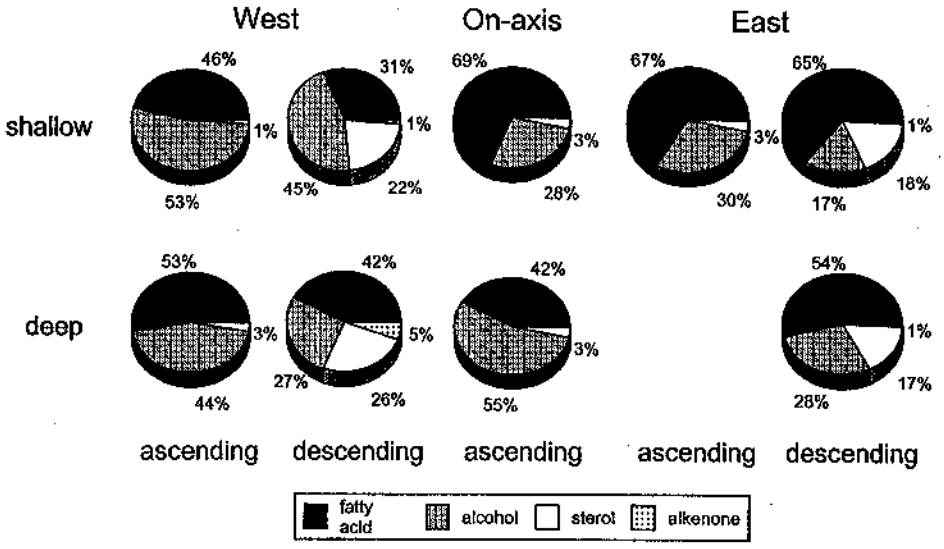

Fig. 9. Fractional concentrations of fatty acids (black), alcohols (hatched), sterols (white) and alkenones (stippled) in shallow and deep, ascending and descending particle trap materials.

3.1.4. *Elemental fluxes*

The elemental flux time-series data will be discussed in detail elsewhere (Bertram et al., in review). Mn and Fe are major constituents of hydrothermal emissions and are diagnostic of hydrothermal input to suspended particulate matter (Campbell, 1991; Feely et al., 1998); whereas Ti is a characteristic indicator of inorganic detrital material with little contribution from hydrothermal precipitates. PMn and PFe fluxes are normalized here to PTi rather than PAl because PAl distributions are hydrothermally influenced (Feely et al., 1994).

The data trends in metal fluxes and elemental ratios suggest hydrothermal input to the descending flux at WS and to the ascending fluxes at both WS and OAS, but not to either ascending or descending flux at ES (Figs. 10–12). Descending PTi flux was greatest at ES for both shallow and deep traps (Fig. 10b). However, whereas shallow descending PMn (Fig. 11b) and PFe (Fig. 12b) flux was still significantly less at WS than at ES ($p < 0.005$ and $p < 0.004$, respectively; equal var.), the deep descending PMn and PFe fluxes at WS were close to (Fe) or slightly greater (Mn) than at ES (not significant). The increase in the flux of PFe, PMn and PTi with increasing depth at ES suggests horizontal transport or resuspension. However, in contrast to WS, which has strong (1.7 and 2.6) depth-related enrichment for both descending Fe (PFe/PTi, $p < 0.03$, equal var.) and Mn (PMn/PTi, $p < 0.003$, unequal var.) fluxes, ES showed no similar enrichment in Fe ($0.95, p > 0.5$, equal var.) and considerably smaller enrichment in Mn ($1.5, p < 0.01$, equal var.) with respect to Ti.

Ascending PMn and PFe fluxes were 1–3 orders of magnitude smaller than descending fluxes (Figs. 11a and 12a). Highest ascending metal fluxes were at OAS, especially the first 3 collection intervals for the deep trap. Deep ascending PFe and PMn flux were significantly greater ($p < 0.05$,

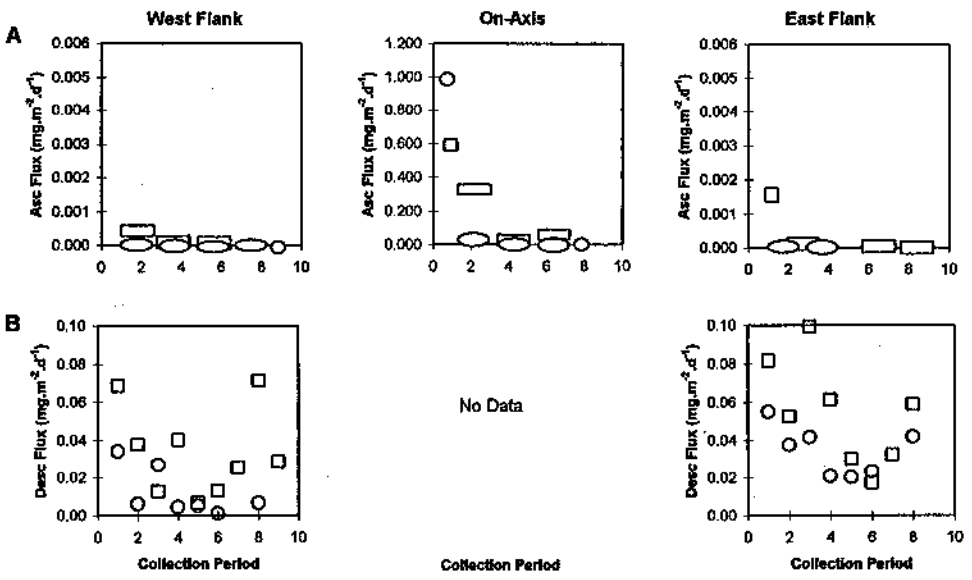

Fig. 10. Time-series particulate Ti fluxes to the shallow (circles, ovals) and deep (squares, rectangles) particle traps moored at the West Flank, on-axis, and East Flank sites: (A) ascending flux; (B) descending flux. Ovals and rectangles represent pooled collection intervals.

unequal var.) at OAS than at either WS or ES. Otherwise, ascending PMn, PFe, and PTi fluxes were generally slightly higher at OAS and WS than at ES for both shallow and deep traps. In general, ascending fluxes were highest in early collection periods (1–3 or July to September), then dropped dramatically.

The average PMn/PTi and PFe/PTi ratios for ascending particles are generally higher at OAS and WS than at ES and for descending particles at WS than at ES (Figs. 11 and 12; Table 2). Highest ascending PMn/PTi ratios were measured for the deep OAS trap and both WS trap depths (Fig. 11c), all of which were significantly greater than corresponding ES traps (deep OAS, $p < 0.02$; shallow WS, $p < 0.007$; deep WS, $p < 0.05$; all unequal var.). Ascending PFe/PTi ratios were also $2\times$ or more higher in deep OAS traps than in either WS ($p < 0.002$, unequal var.) or ES ($p < 0.001$, unequal var.) deep traps (Fig. 12c). Deep descending PFe/PTi and PMn/PTi ratios were $2\times$ greater at WS than ES ($p < 0.02$ and $p < 0.005$, respectively; both unequal var.) (Figs. 11d and 12d). The descending metal ratios to shallow traps were slightly greater at WS than ES, but not significantly so. Shallow ascending OAS metal ratios, on the other hand, were significantly ($p < 0.05$, unequal var.) lower than traps at other depths and sites. The greater variances in the WS trap PMn/PTi and PFe/PTi ratio values relative to the ES values may be related to the meandering nature of the off-axis hydrothermal plume that could result in intermittent delivery of hydrothermal materials to the stationary WS traps. Overall, the elemental data clearly suggest significant hydrothermal input to the descending particle flux at the WS deep trap and to the ascending flux at the OAS deep trap and, possibly, at WS.

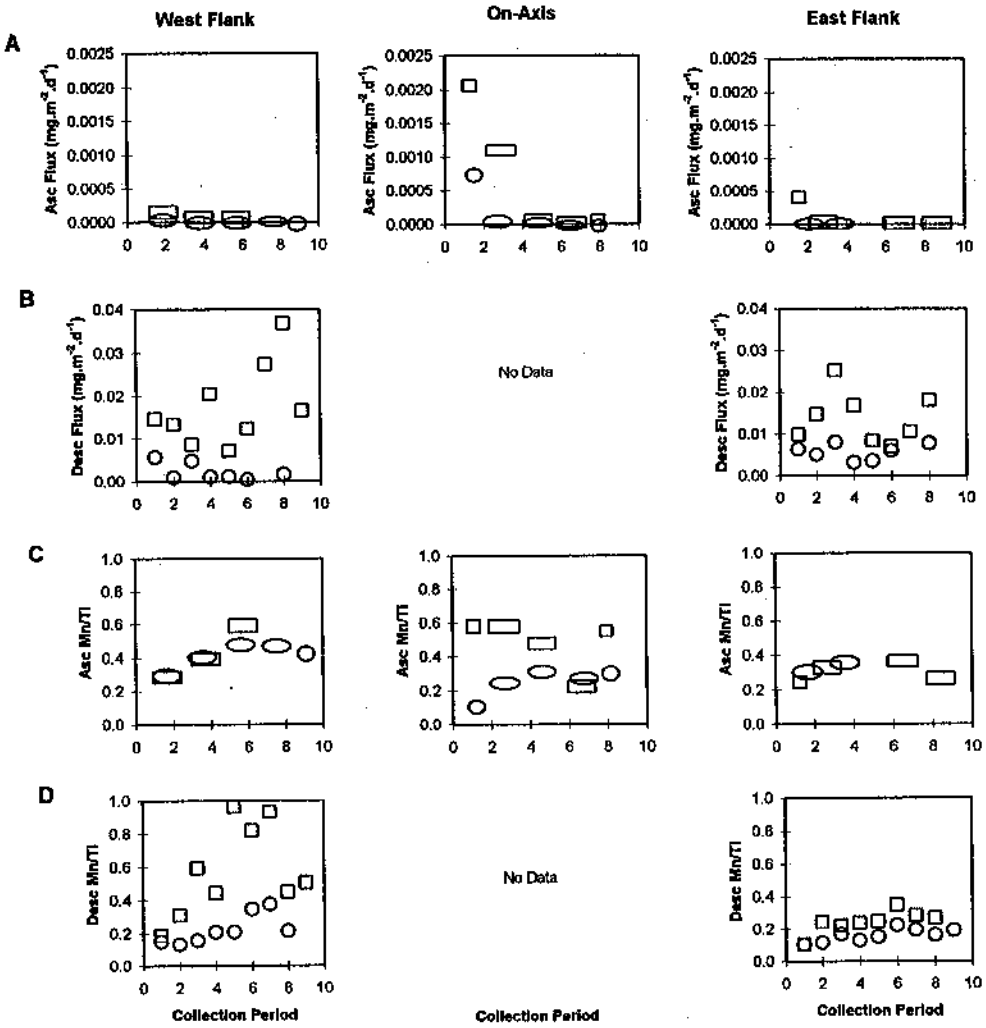

Fig. 11. Time-series particulate Mn fluxes to the shallow (circles, ovals) and deep (squares, rectangles) particle traps moored at the West Flank, on-axis, and East Flank sites: (A) ascending PMn flux; (B) descending PMn flux; (C) ascending particulate PMn:PTi ratios; (D) descending particulate PMn:PTi ratios. Ovals and rectangles represent pooled collection intervals.

4. Discussion

4.1. Ascending flux

Clear signals of ascending flux at all three sites confirm, and extend to the vicinity of mid-ocean ridges, earlier measurements of ascending flux in oceanic settings. Smith et al. (1989) measured the ascending and descending flux at a station within the California Current at 32°50′N and at an

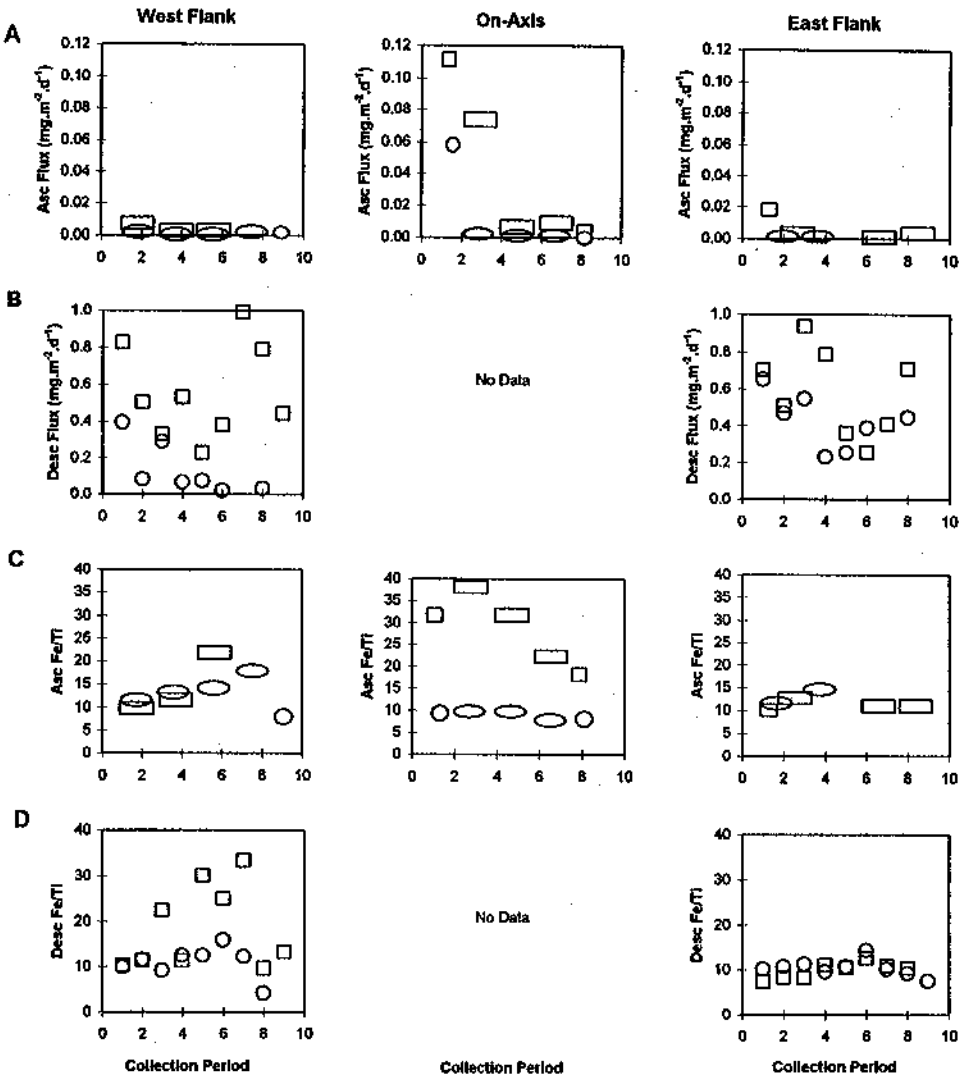

Fig. 12. Time-series particulate Fe fluxes to the shallow (circles, ovals) and deep (squares, rectangles) particle traps moored at the West Flank, on-axis, and East Flank sites. (A) ascending PFe flux; (B) descending PFe flux; (C) ascending particulate PFe : PTi ratios; (D) descending particulate PFe : PTi ratios. Ovals and rectangles represent pooled collection intervals.

oligotrophic central gyre station north of Hawaii at 31°N, 159°W, and Grimalt et al. (1990) observed fluxes at a similar California Current station (~ 39°29.4′N, 127°41.4′W) and at a North Atlantic station over the Hatteras Abyssal Plain, ~ 350 km offshore. Our ascending to descending ratios for TPM are up to 8 times higher than Grimalt, only partly because descending particle fluxes at our sites were within the lower range of values measured by Grimalt (Table 3). Our three stations show higher ascending total particle fluxes than measured in either the Smith or Grimalt

Table 3
Comparison of ascending and descending flux studies

Station	Location	Season	Depth (m)	Total particle flux ($mg\,m^{-2}\,d^{-1}$)			C-flux ($mg\,m^{-2}\,d^{-1}$)		
				Desc.	Asc.	Ratio (A/D)	Desc.	Asc.	Ratio (A/D)
Present study									
West	47°56.4′N;	Avg	1690	6	0.54	0.09	0.84	0.73	0.86
West	129°9.7′W	Avg	2040	25.5	0.27	0.01	1.95	0.39	0.20
On-axis	47°57.0′N	Avg	1661		0.85			0.92	
On-axis	129°5.7′W	Avg	2010		0.83			0.45	
East	48°7.5′N	Avg	1637	27.9	0.47	0.02	4.13	0.56	0.14
East	128°21.1′W	Avg	1986	30.2	0.34	0.01	2.96	0.21	0.07
Smith et al. (1989)									
Sta F	32°50′N	Spr	2800				0.42	0.16	0.38
	124°W	Spr	2800				1.06	0.25	0.24
		Spr	3800				1.03	0.08	0.08
		Spr	3800				1.36	0.13	0.10
		Fall	3800				2.30	0.03	0.01
		Fall	3800				2.03	0.04	0.02
Grimalt et al. (1990)									
NW Pac.	39°29.4′N;	Fall	3800	82.2	0.30	0.004	2.60	0.27	0.10
	127°41.4′W	Sum	3800	41.1	0.45	0.011	1.53	0.38	0.25
NE Atl.	32°46.2′N;	Spr/sum	2865	43.8	0.07	0.002	0.99	0.07	0.07
	70°47.4′W		4700	49.3	0.22	0.004	2.49	0.20	0.08
		Sum/fall	4700	35.6	0.22	0.006	1.45	0.20	0.14
		Fall/win	2850	23.8	0.25	0.010	1.15	0.20	0.17
Roth and Dymond (1989) (2 km NE of Endeavour main vent field)									
NE Pac.	47°58′N	Avg	1700	74.0			3.50		
	129°55.5′W	Avg	1950	34.8			1.60		
		Avg	2178	75.6			2.52		

studies. The present study's POC-flux and carbon content were also generally higher for both descending and ascending traps than either the Smith et al. (1989) or Grimalt et al. (1990) studies, although the ratios for ascending to descending POC-flux are comparable. The highest ascending:descending C-flux ratios for any of the reported studies were measured in the shallow WS traps (note absence of similar data from OAS). The ascending lipid flux and concentrations are also considerably greater than the descending lipid flux. This is expected since the lower specific density of lipids would confer on lipid colloids and lipid-rich particles a tendency toward positive buoyancy.

4.2. *Hydrothermal influence*

A guiding premise for this study was the expectation that hydrothermal systems could exert a measurable influence on ascending and descending POC fluxes. Our limited data are not

conclusive in this regard due in part to the failure of OAS descending particle traps. Nevertheless, intriguing trends in the trap data are consistent with hydrothermal contributions to ascending and descending particle flux. The descending POC and PN fluxes consistently increased from shallow to deep traps at WS (average increase: 0.8–2 mg $m^{-2} d^{-1}$; Table 2), suggesting an input of sinking POC at plume depths. In contrast, no corresponding temporal pattern was observed in the ES descending flux and average POC and PN fluxes decreased slightly, consistent with a surface-derived source of organic-C with subsequent generally depth-related degradation (Suess, 1980). Furthermore, the average ascending carbon fluxes at the shallow (0.9 mg $m^{-2} d^{-1}$) and deep (0.5 mg $m^{-2} d^{-1}$) OAS traps were 1.5–2 times those at the background ES (0.6 and 0.2 mg $m^{-2} d^{-1}$; respectively), with intermediate average WS POC-fluxes (0.7 and 0.4 mg $m^{-2} d^{-1}$; Table 3). Consequently, the highest ascending to descending C-flux ratios were measured at WS. We interpret these trends as suggesting an input of POC from a westward advective component of the hydrothermal plume.

While the highest descending fluxes were found at the more coastal ES, the highest ascending fluxes were found at OAS and WS. The high descending total particulate flux at ES may reflect either a stronger influence from coastal runoff (Peña et al., 1999) or greater productivity at this site, or both. The average descending POC and PN-fluxes decreased from ES (background) to WS, consistent with a diminishing surface productivity and corresponding descending POC flux with increasing distance offshore.

An alternate explanation for some of the differences in particle flux observed among the three sites is random environmental heterogeneity, independent of the hydrothermal system. There are, unfortunately, few particle flux data from mid-ocean ridges (Roth and Dymond, 1989), and no other ascending flux data, with which to compare present results. Roth and Dymond (1989) studied descending POC flux to several traps moored 2 km northeast of the main Endeavour vent field. Their average descending POC flux to a 1700 m trap was ~ 4 times greater than to our shallow WS POC descending trap, but was comparable to our ES shallow trap. Roth and Dymond (1989) also calculated a larger hydrothermal component in traps within or below the plume than found in our deep WS trap (Bertram et al., in review), although total POC flux was similar at these depths in both studies (2.0 in this study versus 1.6–2.5 mg $m^{-2} d^{-1}$ in Roth and Dymond, 1989). Our average shallow WS descending flux may have been anomalously low, with a large range of variability (Table 2). However, the variability of our 8 collection periods is the same magnitude (~ 3 times) as for the 4 seasonal periods sampled during the Roth and Dymond (1989) study. A higher hydrothermal contribution to their deep traps may be well explained by the relative locations of the respective moorings. Our WS mooring was on the ridge flank, 3 km west of the MEF; the Roth and Dymond (1989) mooring was 2 km NE of the MEF, in the vicinity of the High Rise Field, a very active warm and high temperature, axial vent field (Robigou et al., 1993) that was not discovered until after the Roth and Dymond (1989) study.

Hydrothermal influence on the ascending fluxes at OAS and WS, and on descending flux at WS, is supported by the XRF data. Compositionally, the OAS and WS ascending particles are enriched in Fe and Mn relative to background (ES) particles. This is particularly true for PMn in the deep OAS and possibly for the shallow and deep WS traps, and for PFe in the deep OAS traps. It should be recalled that the "deep" traps were deployed within the plumes, and consequently both ascending and descending fluxes could be affected by hydrothermal input at this depth. Ascending PMn and PFe could be associated with fine abiogenic material carried upward with buoyant

ascending organic matter, particles advected horizontally to the traps, or scavenged directly onto organic material.

The deep descending WS trap samples were definitely enriched in both Mn and Fe with respect to the ES deep traps, while the Mn/Ti and Fe/Ti values of WS shallow descending trap samples were generally quite similar to the shallow ES samples. Our data suggest upward transport of plume Fe and Mn at OAS, and possibly at WS, and downward transport of these elements at WS. By extrapolation, we propose that there is likely also hydrothermal input to descending flux at OAS, though these traps failed. Both PMn and PFe have the same West to East pattern in the descending fluxes, with opposite trends for shallow and deep traps. Shallow descending PMn/PTi and PFe/PTi ratios are similar at the ES and WS, while the deep flux ratios are higher at WS, consistent with hydrothermal input (PMn, PFe) to the deep WS traps.

The relatively low PFe/PTi and PMn/PTi ratios found in the shallow OAS trap may be related to this site's close proximity to hydrothermal vent sources and the plume being swept away, down current, before ascending particles could reach shallow trap depths. Alternatively, active grazing by epi-plume zooplankton could greatly reduce the high ascending particle flux indicated by the deep OAS traps, to the low apparent flux measured in the shallow OAS trap. Thomson et al. (1992) consistently observed the highest concentrations of epi-plume zooplankton in the region of OAS.

A variety of sources in hydrothermal systems contribute to POC concentrations and fluxes in the water column. Hydrothermal solutions discharged from focused and diffuse seafloor vents contain organic compounds derived from subsurface microbial and thermochemical processes (Comita et al., 1984; Deming and Baross, 1993). The intense biological communities associated with the vent fields, including surficial seafloor structures (e.g., chimneys, surface sediments) (Karl et al., 1988; Van Dover and Fry, 1994; Delaney et al., 1992; Hannington and Juniper, 1992; Tunnicliffe and Juniper, 1990), also contribute organic carbon through exudation, sloughing, feeding, and export of reproductive products (Comita et al., 1984; Alberic, 1986; Juniper, 1988). In situ production within the buoyant and, especially, the neutrally buoyant plume is another potentially important source of organic carbon (de Angelis et al., 1993; Winn et al., 1995; Cowen et al., 1998).

4.3. *Particle flux and epi-plume zooplankton*

POC production and flux imply that ascending, organic (and lipid)-rich particles could provide a link between the carbon-rich (zooplankton-deficient) zone within the plume and the carbon-poor zone (zooplankton maximum) above the plume. Such a connection would provide plankton access to a hydrothermally enhanced food source and vertically extend the influence of seafloor hydrothermal systems to chemical and biological processes in the upper water column. Secondary production and release of lipid-rich reproductive products (e.g., eggs and larvae) or carcasses from the deep-water acoustic maximum ($\sim$ 1800 m), coupled with vertical migration into the upper water column, would accelerate the exchange of organic carbon and other substances in both directions. Hence, both sinking photosynthetic and rising chemosynthetic-based materials could support local deep and mid-water secondary production. Zooplankton fecal pellets collected by sediment traps deployed within the plume at the Endeavour Ridge can contain both coccolithophorids and sulfide particles, suggesting just such mixed feeding (Dymond and Roth, 1988).

One explanation for the steep vertical gradient in epiplume zooplankton populations is that some subtle density effect occurs there. Elevated concentrations of filamentous and "mucous-like"

material have been observed near the interface of the plume and the above-plume acoustic scattering layer during submersible dives at Endeavour (John Delaney and Marvin Lilley, personal communications). It is conceivable that near-neutrally buoyant sinking and ascending particles are slowed or stopped by weak density discontinuities or changes in small-scale turbulence intensity and vertical velocity at the top of the plume. The former scenario has been observed at shallow water pycnoclines (Costin, 1970; Alldredge and Youngbluth, 1987; Kawakita and Kajihara, 1990), but there is no reported evidence for this in connection with laterally spreading non-buoyant hydrothermal plumes where the density gradient is weaker. However, although vertical profiles of both light attenuation (Fig. 3) and large particles ($> 600\,\mu m$) (Fig. 13) show strong plume maxima, neither shows a maximum at or above the upper plume boundary. Possibly, the portion of the particle population that may be susceptible to slowing at a slight density discontinuity may not be well sampled by nephelometry, photo-imaging, or particle flux traps. Synergistically, if the plume's upper boundary does represent a "stability layer", both rising and sinking particles could accumulate here due to minimum vertical velocities, possibly contributing to the aggregation process (Csanady, 1966; Kawakita and Kajihara, 1990). Vertical velocity of the plume water itself may be a factor only within the strongly buoyant part of the plume.

Alternatively, zooplankton may congregate above the plume simply to intercept ascending particles while avoiding the plume as suggested earlier. A fraction of the zooplankton may also graze at the upper boundary of the large particle maximum found coincident with the plume (Fig. 13). Intense grazing by zooplankton on both suspended and ascending particles near the upper boundary of the plume would reduce the standing stock of food particles and, consequently, reduce the apparent particle flux (i.e., traps). However, the supply of particles is sustained by both vertical and lateral particle fluxes.

4.4. "*Hydrothermal plume*" POC production

Abundant reduced hydrothermal constituents such as hydrogen, methane and ammonia provide potential substrates for chemolithotrophic (and methane oxidation) production of organic carbon within Endeavour plumes (Table 4) (de Angelis et al., 1991, 1993; Winn et al., 1995; McLaughlin, 1998; Cowen et al., 1998). De Angelis et al. (1993) measured methane oxidation rates in Endeavour plumes and estimated that oxidation of vent-derived methane could contribute organic carbon equivalent to 35–150% of that reaching the depth of the plume from surface primary production. Our average measured descending POC flux to traps positioned above the plume (1690 m) at WS was $\sim 1\,mg\,C\,m^{-2}\,d^{-1}$. This is in reasonable agreement with Roth and Dymond (1989), who measured an average descending POC flux of $3.5\,mg\,C\,m^{-2}\,d^{-1}$ at 1700 m at their mooring site. Consequently, integrated hydrothermal methane-derived organic carbon production in the vicinity of the Endeavour plume would be in the range of $0.35–5.4\,mg\,C\,m^{-2}\,d^{-1}$. Based on ammonium concentrations measured in the same Endeavour plume areas and period as covered by the present particle trap results, Cowen et al. (1998) estimated the potential chemolithotrophic production rate of organic carbon derived from hydrothermal vent NH_4^+ to be $0.2–0.9\,mg\,C\,m^{-2}\,d^{-1}$. The latter values assume a 50:50 partitioning of the NH_4^+ between assimilation and oxidation processes (Cowen et al., 1998). A production rate from microbial oxidation of H_2 ($1–2\,mg\,C\,m^{-2}\,d^{-1}$) was derived from H_2 concentrations and oxidation rate experiments measured with Endeavour plume water (Lilley et al., 1993; McLaughlin, 1998).

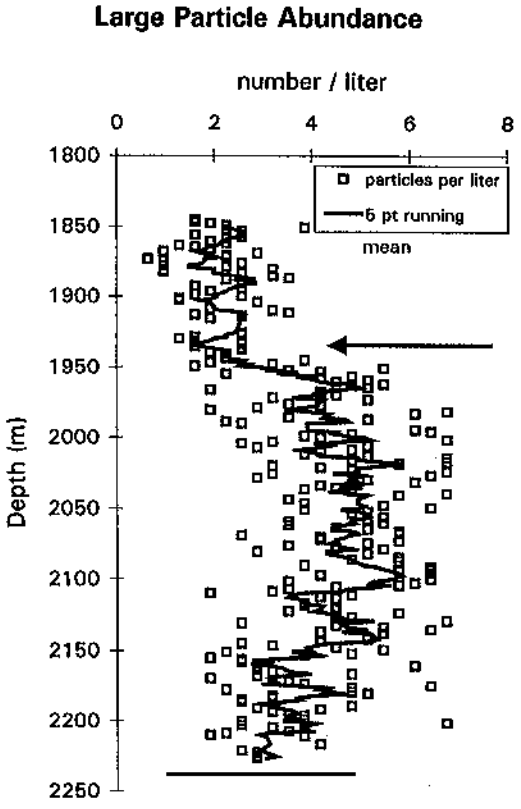

Fig. 13. Vertical profile of large (> 600 μm) particles recorded in Endeavour on-axis plume using an in situ large particle profiling camera and collimated light. Both individual data points (open squares) and a 5 point running mean (solid line) are shown. Arrow indicates top of hydrothermal plume and the grey line the approximate seafloor depth.

Although the ascending carbon fluxes measured at OAS and WS and descending carbon fluxes at WS must be used with caution, the values compare well with the above estimates of potential organic-carbon production sources associated with the Endeavour Segment hydrothermal plumes (Table 4). Organic carbon production terms would change with plume "age" (i.e., down-current) as the specific oxidation rates change (i.e., as bacterial populations evolve) and substrate concentrations decrease. Nevertheless, the lower range of the estimated total organic carbon production rate (1.7–9 mg C m^{-2} d^{-1}) within the plume from hydrothermally derived reduced substrates is comparable to the descending organic carbon fluxes (1–4 mg C m^{-2} d^{-1}) derived from photosynthesis at the ocean surface that reaches plume depths. Significantly, the plume's in situ organic carbon production alone could account for the estimated total hydrothermally derived flux (ascending plus descending) out of the plume (1.5–2.5 mg C m^{-2} d^{-1}) plus additional postulated zooplankton grazed POC. Furthermore, the labile nature of this fresh organic carbon relative to the more refractory ambient deep-water organic carbon underscores the potential significance to feeding zooplankton (Comita et al., 1984; Roth and Dymond, 1989; Khirpounoff and Alberic, 1991; de Angelis et al., 1993; Winn et al., 1995). The relative consumption rates of hydrothermal-derived

Table 4
Inventory of potential sources of organic-C production and fluxes to/from Endeavour plume[a]

Principal process	Total org-C ($mg C m^{-2} d^{-1}$)	"Hydroth" component ($mg C m^{-2} d^{-1}$)	"Surface" component ($mg C m^{-2} d^{-1}$)
In situ production			
NH_4^+ oxid[b]	0.2–0.9	0.2–0.9	—[c]
CH_4 oxid[d]	0.4–6	0.4–6	—
H_2 oxid[e]	1–2	1–2	—
In situ $S^=$ oxid[f]	~0.1	~0.1	—
Entrained "hydroth. prod."	?	?	—
Total	> 1.7–9	> 1.7–9	—
Above plume			
Ascending flux	0.9	0.5[h]	'0.4'
Descending flux[g]	1–(4)[g]	0	1–(4)[g]
Base of plume			
Ascending flux	0.4	'0'	'0.3'
Descending flux	2–4	1–2[i]	1–2[i]
Tot. "hydrothermal" particle flux from plume		(1.5)–2.5	
Hydroth. flux to epi-plume depth (asc)		0.5	
"Surface" flux to epi-plume depth (asc + desc)			1.4–(4.4)
Total flux to epi-plume depths	1.9–4.9		

[a]Data derived from present study except where noted.
[b]Cowen et al., 1998.
[c]"–"indicates negligible quantities.
[d]De Angelis et al. (1993); Lilley et al. (1993).
[e]Derived from McLaughlin (1998) and Lilley et al. (1993).
[f]Winn et al. (1995).
[g]High end of range from Roth and Dymond (1989), low end of range from present study.
[h]Calculated as difference between this study's average shallow and deep ascending traps. Conservative in sense that "deep" trap were within plume, not at base or below plume. Conservatively assumes deep traps in present study were at base of plume; uses deep trap flux from West Flank site.
[i]Based on Roth and Dymond (1989) estimate that 50% of descending C-flux at base of Endeavour plume derived from "hydrothermal" input.

POC versus surface (photosynthesis) derived POC are unknown. The latter will vary qualitatively and quantitatively with season from a fine rain of relatively refractory material to the rapid fallout of more labile material following a plankton bloom. Indeed, periods of low ascending flux at the Endeavour site may be due to a draw-down effect from high surface productivity, high descending flux period (Bertram et al., in review).

4.5. Zooplankton energy requirements versus hydrothermal organic carbon

Finally, it is constructive to consider the magnitude of potential carbon production in, and exports from, the hydrothermal plume with respect to the estimated organic carbon requirements

Table 5
Organic carbon flux 'required' to support epi-plume zooplankton anomaly at endeavour segment

Zooplankton biomass (total dry wt), integrated 100 m above plume		$\sim 500\,mg\,m^{-2}$	Burd et al. (1992)
Zooplankton C-content as % total dry wt.			Omari (1969)
Crustacia[a]	40–53%		
Chaetognaths[a]	46%		
Pisces[a]	42%		
Fraction of total dry wt as carbon: $500\,mg\,m^{-2} \times 0.45 =$		$\sim 225\,mg\,C\,m^{-2}$	
Zooplankton daily Productivity : Standing Crop ratio:			Mullin (1970)
Barents Sea	$0.002\,d^{-1}$		
NW Pacific (summer)	$0.01\,d^{-1}$		
NE Pacific (year)	$0.008\,d^{-1}$		
Epi-plume zooplankton production: $225\,mg\,C\,m^{-2} \times 0.01\,d^{-1} = 2.2\,mg\,C\,m^{-2}\,d^{-1}$			
$225\,mg\,C\,m^{-2} \times 0.002\,d^{-1} = 0.5\,mg\,C\,m^{-2}\,d^{-1}$			
"Required" org.-C input (assuming 10% 'food' conversion factor):		$5–22\,mg\,C\,m^{-2}\,d^{-1}$	
"Surface" (photosyn.) particle flux to 1700 m: $1.3–4.3\,mg\,C\,m^{-2}\,d^{-1}$			
Ascending "hydrothermal" flux: $0.5\,mg\,C\,m^{-2}\,d^{-1}$			
Total flux to epi-plume depths:		$2–5\,mg\,C\,m^{-2}\,d^{-1}$	
Potential in situ 'plume' production:		$2–9\,mg\,C\,m^{-2}\,d^{-1}$	

[a]These 3 zooplankton groups comprise 90% of epi-plume zooplankton congregation.

of the anomalous zooplankton congregations observed above the plume at the Endeavour segment. In Table 5 we back-calculate to the daily organic-C input "required" to support the zooplankton biomass integrated over the 100 m depth range of a typical zooplankton anomaly found just above the Endeavour plume. Starting with ~ 500 mg (dry) zooplankton m^{-2} (Burd et al., 1992) and applying an average dry weight to carbon conversion factor of 0.45 (Omari, 1969), we estimate a total dry weight of $225\,mg\,C\,m^{-2}$ for the standing biomass of zooplankton. Measurements for the ratio of zooplankton daily production to standing biomass vary over an order of magnitude ($0.002–0.01\,d^{-1}$) for areas in the North Pacific and Barents Sea (Mullin, 1970). Applying these production:biomass ratios to the epi-plume zooplankton biomass yields a range of $0.5–2.2\,mg\,C\,m^{-2}\,d^{-1}$ for daily zooplankton production. Assuming a "food-substrate" conversion factor of 10% yields a "required" organic carbon source of $5–22\,mg\,C\,m^{-2}\,d^{-1}$ to sustain the integrated biomass measured in the epi-plume zooplankton anomaly at Endeavour.

These simple bio-energetic calculations assume direct transfer of the particulate carbon flux to zooplankton biomass. They also do not consider the effect of undetected rapid migrations by zooplankton into and out of the hydrothermal plume that would effectively increase access to hydrothermal plume organic carbon production. Nevertheless, the calculated range for required organic carbon input is remarkably similar to the estimates of both the total flux to epi-plume depths (combined hydrothermal and surface-derived organic carbon; $2–5\,mg\,C\,m^{-2}\,d^{-1}$, Table 5) and of the potential total plume in situ organic carbon production ($1.7–9\,mg\,C\,m^{-2}\,d^{-1}$; Tables 4 and 5).

Acknowledgements

We thank Hugh Milburn for modifications to the PMEL sediment traps and the officers and crew of the Canadian research vessels *CFAV Endeavour* and *CSS J.P. Tulley* and the NOAA ship *R.V. Surveyor* for their excellent ship handling and support. We gratefully acknowledge the shipboard and laboratory technical help of Reg Bingham, Charles Holloway, Donald McGee, Bernard Minkley, David Tennant, Les Spearing, Rachel Shackelford, Wendy Smith, Geoff Lebon, and Xiyuan Wen. Geoff Wheat and Joseph Resing generously shared their analytical expertise for Mn and Fe analyses. Two anonymous reviewers provided extraordinarily detailed and helpful comments. The study was supported by NSF (OCE-9416560 and OCE9618121 to JPC, and OCE-9310364 to SGW), Canadian Fisheries Service, and the NOAA VENTS Program. This is SOEST contribution no. 5225 and PMEL contribution no. 2092.

References

Alberic, P., 1986. Composition en acides amines des particules en suspension des events hydrothermaux (dorsale Est-Pacifique 13°N). Oceanologia Acta 9, 73–79.

Alldredge, A.L., Youngbluth, M.J., 1987. The significance of macroscopic aggregates (marine snow) as sites for heterotrophic bacterial production in the mesopelagic zone of the subtropical Atlantic. Deep-Sea Research 32, 1445–1456.

Baker, E.T., Milburn, H.B., 1983. An instrument system for the investigation of particle fluxes. Continental Shelf Research 1, 425–435.

Baker, E.T., Piper, D.Z., 1976. Suspended particulate matter: collection by pressure filtration and elemental analysis by thin film X-ray fluorescence. Deep-Sea Research 23, 181–186.

Bertram, M.A., Cowen, J.P., Thomson, R.E., Feely, R.A., Compositional variability in the ascending and descending fluxes from a hydrothermal plume. Journal of Geophysical Research, in review.

Bolger, G.W., Betzer, P.R., Gordon, V., 1978. Hydrothermally derived manganese suspended over the Galapagos spreading center. Deep-Sea Research 25, 721–733.

Burd, B.J., Thomson, R.E., 1993. Flow volume calculations based on three-dimensional current and net orientation data. Deep-Sea Research 40, 1141–1153.

Burd, B.J., Thomson, R.E., Jamieson, G.S., 1992. Composition of a deep scattering layer overlying a mid-ocean ridge hydrothermal plume. Marine Biology 113, 517–526.

Campbell, A.C., 1991. Mineralogy and chemistry of marine particles by synchrotron X-ray spectrometry, Mossbauer spectrometry, and plasma-mass spectrometry. In: Hurd, D.C., Spencer, D.W. (Eds.), Marine Particles: Analysis and Characterization, Geophysical Monographs Series, Vol. 63. AGU, Washington, D.C., pp. 375–390.

Cannon, G.A., Pashinski, D.J., 1997. Variations in mean currents affecting hydrothermal plumes on the Juan de Fuca Ridge. Journal of Geophysical Research 102, 24965–24976.

Comita, P.B., Gagosian, R.B., Williams, P.M., 1984. Suspended particulate organic material from hydrothermal vent waters at 21°N. Nature (London) 307, 450–453.

Costin, J.M., 1970. Visual observations of suspended-particle distribution at three sites in the Caribbean Sea. Journal of Geophysical Research 75, 4144–4150.

Cowen, J.P., Massoth, G.J., Baker, E.T., 1986. Bacterial scavenging of Mn and Fe in a mid- to far-field hydrothermal particle plume. Nature 322, 169–171.

Cowen, J.P., Massoth, G.J., Feely, R.A., 1990. Scavenging rates of dissolved manganese in a hydrothermal vent plume. Deep-Sea Research 37, 1619–1637.

Cowen, J.P., Wen, X., Jones, R.D., Thomson, R.E., 1998. Elevated NH_4^+ in neutrally-buoyant hydrothermal plume: Endeavour Segment, Juan de Fuca Ridge. Deep-Sea Research I 45, 1891–1902.

Csanady, G.T., 1966. Accelerated diffusion in the skewed shear flow of lake currents. Journal of Geophysical Research 71, 411–420.

DeAngelis, M.A., Baross, J.A., Lilley, M.D., 1991. Enhanced microbial methane oxidation in water from a deep-sea hydrothermal vent field at simulated in situ hydrostatic pressures. Limnology and Oceanography 36, 565–570.

DeAngelis, M.A., Lilley, M.D., Olson, E.J., Baross, J.A., 1993. Methane oxidation in deep-sea hydrothermal plumes of the Endeavour Segment of the Juan de Fuca Ridge. Deep-Sea Research 40, 1169–1186.

Delaney, J.R., Kelley, D.S., Lilley, M.D., Butterfield, D.A., McDuff, R.E., Baross, J.A., Deming, J.W., Johnson, H.P., Robigou, V., 1997. The Endeavour hydrothermal system I: cellular circulation above an active cracking front yields large sulfide structures, "fresh" vent water, and hyperthermophilic Archaea. RIDGE Events 8, 11–19.

Delaney, J.R., Robigou, V., McDuff, R.E., Tivey, M.K., 1992. Geology of a vigorous hydrothermal system on the Endeavour Segment, Juan de Fuca Ridge. Journal of Geophysical Research 97, 19663–19682.

Deming, J.W., Baross, J.A., 1993. Deep-sea smokers: windows to a subsurface biosphere? Geochimica et Cosmochimica Acta 57, 3219–3230.

Dymond, J., Roth, S., 1988. Plume dispersed hydrothermal particles: a time-series record of settling flux from the Endeavour Ridge using moored sensors. Geochimica et Cosmochimica Acta 52, 2525–2536.

Feely, R.A., Baker, E.T., Lebon, G.T., Gendron, J.F., Massoth, G.J., Mordy, C.W., 1998. Chemical variations of hydrothermal particles in the 1996 Gorda Ridge event and chronic plumes. Deep-Sea Research II 45, 2637–2664.

Feely, R.A., Massoth, G.J., Baker, E.T., Lebon, G.T., Geiselman, T., 1992. Tracking the dispersal of hydrothermal plumes from the Juan de Fuca Ridge using suspended matter compositions. Journal of Geophysical Research 9, 3457–3468.

Feely, R.A., Massoth, G.J., Lebon, G.T., 1991. Sampling of marine particulate matter and analysis by X-ray fluorescence spectrometry. In: Hurd, D.C., Spencer, D.W. (Eds.), Marine Particles: Analysis and Characterization, Geophysical Monographs Series, Vol. 63. AGU, Washington, D.C., pp. 251–257.

Feely, R.A., Massoth, G.J., Trefry, J.H., Baker, E.T., Paulson, A.J., Lebon, G.T., 1994. Composition and sedimentation of hydrothermal plume particles from North Cleft segment, Juan de Fuca Ridge. Journal of Geophysical Research 99, 4985–5006.

Grimalt, J.O., Simoneit, B.R.T., Gomez-Belinchon, J.I., Fischer, K., Dymond, J., 1990. Ascending and descending fluxes of lipid compounds in North Atlantic and North Pacific abyssal waters. Nature 345, 147–150.

Gust, G., Michaels, A.F., Johnson, R., Deuser, W.G., Bowles, W., 1994. Mooring line motions and sediment trap hydromechanics: in situ inter-comparison of three common deployment designs. Deep-Sea Research I 41, 831–857.

Hannington, M., Juniper, K., 1992. The ecology and geological evolution of large sulfide structures: scaling up from chimney models. Ridge Research Report 3, 38.

Holmes, G.S., 1981. The limitations of accurate 'thin-film' X-ray fluorescence analysis of natural particulate matter: problems and solutions. Chemical Geology 33, 333–353.

Jones, R.D., 1991. An improved fluorescence method for the determination of nanomolar concentrations of ammonium in natural waters. Limnology and Oceanography 36, 814–819.

Juniper, S.K., 1988. Geochimie et ecologie d'unmicroenvironnement hydrothermal, les secretions de mucus de Paralvinella palmiformis. Oceanology Acta (Spec.) 8, 167–172.

Karl, D.M., Christian, J.R., Dore, J.E., Hebel, D.V., Letelier, R.M., Tupas, L.M., Winn, C.D., 1996. Seasonal and interannual variability in primary production and particle flux at Station Aloha. Deep-Sea Research II 43, 539–568.

Karl, D.M., Taylor, G.T., Novitsky, J.A., Jannasch, H.W., Wirsen, C.O., Pace, N.R., Lane, D.J., Olsen, G.J., Giovannoni, S.J., 1988. A microbiological study of Guaymas Basin high temperature hydrothermal vents. Deep-Sea Research 35, 777–791.

Kawakita, K., Kajihara, M., 1990. Effects of static stability and the C/N ratio on aggregation processes of oceanic particles. Journal of the Oceanographical Society of Japan 46, 1–8.

Khirpounoff, A., Alberic, P., 1991. Settling of particles in a hydrothermal vent field (East Pacific Rise 13°N) measured with sediment traps. Deep-Sea Research 38, 729–744.

Klinkhammer, G.P., Hudson, R., 1987. Dispersal patterns for hydrothermal plumes in the southern Pacific using manganese as a tracer. Earth and Planetary Science Letters 79, 241–249.

Knauer, G.A., Asper, V., 1989. Sediment trap technology and sampling. U.S. GOFS Planning Report 10, U.S. GOFS Planning Office, Woods Hole, Massachusetts, 94pp.

Knauer, G.A., Karl, D.M., Martin, J.H., Hunter, C.N., 1984. In situ effects of selected preservatives on total carbon, nitrogen and metals collected in sediment traps. Journal of Marine Research 42, 445–462.
Lavelle, J.W., Cowen, J.P., Massoth, G., 1992. A model for the deposition of hydrothermal manganese near ridge crests. Journal of Geophysical Research 97, 7413–7427.
Lilley, M.D., Butterfield, D.A., Olson, E.J., Lupton, J.E., Macko, S.E., McDuff, R.E., 1993. Anomalous CH_4 and NH_4^+ concentrations at an unsedimented mid-ocean ridge hydrothermal system. Nature 364, 45–47.
Lilley, M.D., Landsteiner, M.C., McLaughlin, E.A., Parker, C.B., Cherkaoui, A.S.M., Lebon, G., Viers, S.R., Delaney, J.R., 1995. Real-time mapping of hydrothermal plumes on the Endeavour Segment of the Juan de Fuca. EOS Transactions of the American Geophysical Union 76, 420.
Lupton, J.E., Klinkhammer, G.P., Normark, W.R., Haymon, R., MacDonald, K.C., Weiss, R.F., Craig, H., 1980. Helium-3 and manganese at the 21°N East Pacific Rise hydrothermal site. Earth and Planetary Science Letters 50, 1149–1161.
McLaughlin, E.A., 1998. Microbial hydrogen oxidation associated with deep-sea hydrothermal vent environments. Ph.D. Dissertation, University of Washington.
Mihaly, S.F., Thomson, R.E., Rabinovich, A.B., 1998. Evidence for nonlinear interaction between internal waves of inertial and semidiurnal frequency. Geophysical Research Letters 25, 1205–1208.
Mullin, M., 1970. Production of zooplankton in the ocean: the present status and problems. Oceanography and Marine Biology Annual Review 7, 293–314.
Omari, M., 1969. Weight and chemical composition of some important oceanic zooplankton in the North Pacific Ocean. Marine Biology 3, 4–10.
Peña, M.A., Denman, K.L., Calvert, S.E., Thomson, R.E., Forbes, J.R., 1999. The seasonal cycle in sinking particle fluxes off Vancouver Island, British Columbia. Deep-Sea Research II 46, 2969–2992.
Popp, B.N., Sansone, F.J., Rust, T.R., Merritt, D.A., 1995. Determination of concentration and carbon isotopic composition of dissolved methane in sediments and nearshore waters. Analytical Chemistry 34, 405–411.
Resing, J.A., Mottl, M.J., 1992. Determination of manganese in seawater using flow injection analysis with on-line preconcentration and spectrophotometric detection. Analytical Chemistry 64, 2682–2687.
Robigou, V., Delaney, J.R., Stakes, D., 1993. The High-Rise hydrothermal vent field, Endeavour Segment, Juan de Fuca Ridge. Geophysical Research Letters 20P, 1887–1890.
Roth, S.E., Dymond, J., 1989. Transport and settling of organic material in a deep-sea hydrothermal plume: evidence from particle flux measurements. Deep-Sea Research 36, 1237–1254.
Sansone, F.J., Popp, B.N., Rust, T.M., 1997. Stable carbon isotopic analysis of low-level methane in water and gas. Analytical Chemistry 69, 40–44.
Simoneit, B.R.T., Grimalt, J.O., Fischer, K., Dymond, J., 1986. Upward and downward flux of particulate organic material in abyssal waters of the Pacific Ocean. Naturwissenschaften 73, 322–325.
Smith, K.L., Williams, P.M., Druffel, E.R.M., 1989. Upward fluxes of particulate organic matter in the deep North Pacific. Nature 337, 724–726.
Suess, E., 1980. Particulate organic carbon flux in the oceans — surface productivity and oxygen utilization. Nature, London 288, 260–263.
Tennant, D.A., Baker, E.T., 1987. A fast, high-precision splitter for particle suspensions. Marine Geology 108, 247–252.
Thomson, R.E., Burd, B.J., Dolling, A.G., Gordon, R.L., Jamieson, G.S., 1992a. The deep scattering layer associated with the Endeavour Ridge hydrothermal plume. Deep-Sea Research 39, 55–73.
Thomson, R.E., Delaney, J.R., McDuff, R.E., Janecky, D.R., McCain, J.S., 1992b. Physical characteristics of the Endeavour Ridge hydrothermal plume during July 1998. Earth and Planetary Science Letters 111, 141–154.
Thomson, R.E., Gordon, R.L., Dolling, A.G., 1991. An intense acoustic scattering layer at the top of a mid-ocean ridge hydrothermal plume. Journal of Geophysical Research 96, 4839–4844.
Thomson, R.E., Gordon, R.L., Dymond, J., 1988. Remote observations of hydrothermal vents. Sea Technology 29, 17–19.
Thomson, R.E., Gordon, R.L., Dymond, J., 1989. Acoustic doppler current profiler observations of a mid-ocean ridge hydrothermal plume. Journal of Geophysical Research 94, 4709–4720.
Thomson, R.E., LeBlond, P.H., Rabinovich, A.B., 1998. Satellite-tracked drifter measurements of inertial and semidiurnal currents in the northeast Pacific. Journal of Geophysical Research 103 (1), 1039–1071.
Tunnicliffe, V., 1991. The biology of hydrothermal vents: ecology and evolution. Oceanography and Marine Biology Annual Review 29, 319–407.

Tunnicliffe, V., Juniper, S.K., 1990. Dynamic character of the hydrothermal vent habitat and the nature of sulfide chimney fauna. Progress in Oceanography 24, 1–13.

Van Dover, C.L., Fry, B., 1989. Stable isotopic compositions of hydrothermal vent organisms. Marine Biology 102, 257–262.

Van Dover, C.L., Fry, B., 1994. Microorganisms as food resources at deep-sea hydrothermal vents. Limnology and Oceanography 39, 51–57.

Veirs, S.R., Landsteiner, M.C., Lilley, M.D., 1996. CTDT characterization of ridge crest hydrothermal activity. EOS 77, F404.

Von Damm, K.L., 1990. Seafloor hydrothermal activity: Black smoker chemistry and chimneys. Annual Revew of Earth and Planetary Science 18, 173–204.

Wakeham, S.G., Canuel, E.A., 1988. Organic geochemistry of particulate matter in the eastern tropical North Pacific Ocean: Implications for particle dynamics. Journal of Marine Research 46, 183–213.

Wakeham, S.G., Lee, C., Farrington, J.W., Gagosian, R.B., 1984. Biogeochemistry of particulate organic matter in the oceans — results from sediment trap experiments. Deep-Sea Research 31, 509–528.

Wetzler, M.A., Lavelle, J.W., Cannon, G.A., Baker, E.T., 1998. Variability of temperature and currents measured near Pipe Organ hydrothermal vent sites. Marine Geophysical Research 20 (6), 505–516.

Wiebe, P.H., Copley, N., Van Dover, C., Tamse, A., Manrique, F., 1988. Deep-water zooplankton of the Guaymas Basin hydrothermal vent field. Deep-Sea Research 35, 985–1013.

Winn, C.D., Cowen, J.P., Karl, D.M., 1995. Microbiology of hydrothermal plumes. In: Karl, D.M. (Ed.), Microbiology of Deep-Sea Hydrothermal Vent Habitats, CRC Press, Boca Raton, pp. 255–274.

Yayanos, A.A., Nevenzel, J.C., 1978. Rising-particle hypothesis: rapid ascent of matter from the deep ocean. Naturwissenschaften 65, 255–256.